1
Preparation of Monolayer Modified Electrodes

Encyclopedia of Electrochemistry. Edited by A.J. Bard and M. Stratmann
Vol. 10 *Modified Electrodes*. Edited by M.Fujihira, I.Rubinstein, and J.F.Rusling
 ISBN: 978-3-527-30402-8

1.1 Modification of Transparent Conducting Oxide (TCO) Electrodes through Silanization and Chemisorption of Small Molecules

Michael Brumbach and Neal R. Armstrong
University of Arizona, Tucson, Arizona

1.1.1 Introduction

1.1.1.1 The Metal Oxide Electrode and Modification Schemes

Surface modification of transparent conducting oxide (TCO) thin film electrodes (indium–tin oxide (ITO), SnO_2, TiO_2, ZnO, etc.) has traditionally been directed toward enhancement of heterogeneous electron transfer rates of solution species for which the electron transfer process is thermodynamically favored but kinetically inhibited. The surface-confined molecule is intended to exhibit rapid and reversible electron transfer at the oxide surface to provide rapid mediation of electron transfer to a solution species [1]. Surface-confined molecules are typically not directly ''wired'' into the conduction or valence band of the oxide, but electron transfer rates are often reasonably fast for these species simply because they have been brought into close proximity to the electronically active sites of the metal oxide. Chemical modification of the TCO surface can be accomplished through covalent bond formation (silanization) or through chemisorption of molecules containing functional groups such as carboxylic acids, phosphonic acids, alkanethiols, and amines.

Initial modification strategies were employed for oxidation of biomolecules, such as ascorbic acid, neurotransmitters, heme proteins, and so forth using various surface-confined molecules or thin films of conducting polymers. Modification schemes have also been used to attach photoactive dye molecules, such as phthalocyanines, porphyrins, and a variety of organometallic complexes, to oxide surfaces to enhance redox processes between solution species and semiconducting electrodes [2–6]. Chemical modification of conducting oxide surfaces has also been used to enhance charge injection rates into condensed phase organic thin film devices (for example, in organic light emitting diodes (OLEDs) and organic photovoltaics (OPVs)). There is still some debate as to whether the enhancement in device performance is due to enhancements in wettability of the oxide surface toward the nonpolar molecules used in these devices, to changes in work function of the oxide surface, and/or to enhancements in

Encyclopedia of Electrochemistry. Edited by A.J. Bard and M. Stratmann
Vol. 10 *Modified Electrodes*. Edited by M.Fujihira, I.Rubinstein, and J.F.Rusling
 ISBN: 978-3-527-30402-8

intrinsic rates of charge injection [7–13]. Many of the same strategies initially used to enhance solution electron transfer rates on these oxide surfaces appear to positively impact device efficiencies in simple OLEDs and OPVs [9, 14–18].

1.1.1.2 Commonly Encountered TCO Electrodes

The most commonly encountered TCO electrodes, typically studied as thin films, are antimony-doped tin oxide (ATO) or fluorine-doped tin oxide (FTO), ITO, titanium oxide (anatase or rutile, TiO_2), and zinc oxide (ZnO) [19]. There are also some recently reported trinary and ternary oxides based on modifications of ITO, zinc-indium tin oxide, ZITO or IZTO, for example, which may become more popular with time as electrodes for solution-based redox chemistry and as anodes in devices such as OLEDs and OPVs [7]. These new tailored composition oxides may exhibit higher stability, higher work functions, and/or a greater variety of surface sites with more possibilities for chemical modification.

An idealized metal oxide surface is shown in Fig. 1, where the metal atoms are in tetrahedral coordination with four oxygen atoms. This metal oxide, empirical formula MO_x, is stoichiometric, having no defects or surface hydrolysis products, and can be considered as a typical platform for understanding the modification of most TCO thin film materials of electrochemical interest. TCO films are typically deposited by sputtering, chemical vapor deposition, or pulsed laser deposition, and tend to be ''microcrystalline'' whose dominant exposed faces tend to be either ⟨111⟩ or ⟨100⟩ lattice terminations [19–23]. The structure and electronic properties of several TCO films can be summarized as follows:

Indium–Tin Oxide (ITO): ITO has the complex unit cell of indium oxide (bixbyite lattice) consisting of more than 80 atoms. Indium oxide has two distinct indium sites in the lattice and as many as four oxygen species, considering surface hydrolysis products and oxygen vacancies [24]. Oxygen vacancies and electron-rich interstitial tin dopant sites lie close in energy to the conduction band edge so that promotion of electrons into the conduction band, at room temperature, is facile [25]. Figure 2 shows the proposed band diagram for ITO exhibiting the common features that dictate the electrical properties of many TCO materials. The upper portion of the valence band arises from filled O(2p) orbitals, while the lower part of the conduction band arises from unfilled metal orbitals (In(5s) orbitals in the case of ITO). Oxygen defects are induced into the TCO material during its formation, usually by depositing or annealing the thin film in an oxygen-deficient atmosphere, thus creating electron-rich sites within a few kT of the conduction band edge. An interstitial dopant, tin, is often introduced into these In_2O_3 lattices at concentrations up to 10% (atomic), producing additional electron-rich sites within a few kT of the conduction band edge. In ITO, the donor density can be as high as 10^{20} cm^{-3} with a sheet resistance as low as 10 Ω sq^{-1}. The introduction of oxygen defect sites and other dopants, however, may also increase the chemical reactivity of these oxide surfaces toward hydrolysis

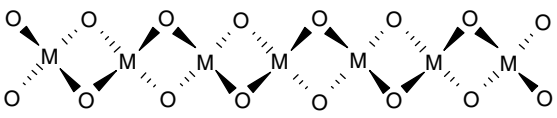

Fig. 1 Schematic view of an ideal metal oxide surface.

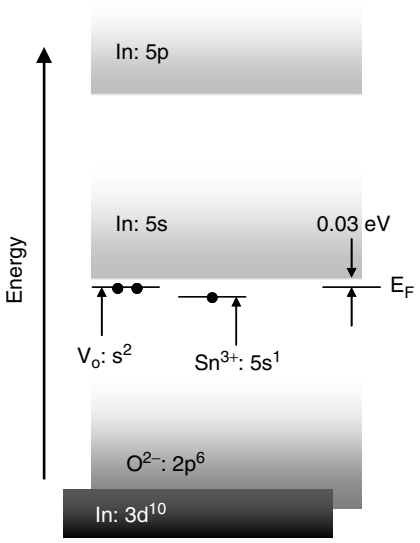

Fig. 2 Schematic view of the energy levels in ITO showing the components of the valence band and conduction band regions of the oxide, the presence of oxygen defect sites and interstitial tin dopant sites that contribute to electron density near the conduction band edge, rendering the oxide conductive at room temperature (after Ref. 25).

and other components of the vacuum deposition system. The reactivity of the oxide surface has important consequences for their further modification and enhancement of electron transfer rates, which have been extensively studied as functions of surface pretreatment [8, 24, 26, 27].

Tin Oxide (SnO_2): Tin oxide has a tetragonal rutile structure with a unit cell of six atoms. The electrical conductivity of n-doped SnO_2 is due to the presence of oxygen vacancies, interstitial tin (in excess), or added dopants such as fluorine, chlorine, or antimony. Carrier concentrations can be increased to approximately 10^{20} cm^{-3} through doping from the intrinsic concentration of approximately 10^{18} cm^{-3} for SnO_2 [19].

Titanium Oxide (TiO_2): Titanium oxide exists in three different crystallographic structures, rutile, anatase, and brookite. The most commonly studied material is rutile, being the most stable phase, although many studies have been conducted on the anatase phase as well [28]. Stoichiometric rutile contains Ti^{4+} in six-fold coordination with oxygen staggered by Ti^{4+} in five-fold coordination. Oxygen atoms at the surface are often bridging and only two-fold coordinated [23]. The band gap of rutile is 3.0 eV, and 3.2 eV for anatase, making titanium oxide a useful material for photocatalysis [29–31]. Photoelectrochemical cells based on sintered nanoparticulate arrays of anatase or thin film TiO_2 electrodes have been quite successful [32, 33]. Both anatase and rutile forms of TiO_2 are readily n-doped by creation of oxygen vacancies leaving electron-rich Ti^{3+} and Ti^{2+} states in the band gap, with electron energies sufficiently close to the conduction band edge so as to provide for reasonable room temperature conductivity.

1.1.1.3 Variability in TCO Electrodes

TCO thin films can exhibit tremendous variability in transparency, microstructure (and surface roughness), surface composition, conductivity, chemical stability at high current densities (in OLEDs, OPVs, and chemical sensors), and in their chemical compatibility with contacting organic layers. Variability is often noticeable from production batch to production batch and within batches of the same metal oxide material [34]. Surface pretreatment conditions have also been shown to dramatically impact the electrochemical, physical, and photophysical properties of metal oxide films [8, 9, 24, 26, 27, 35]. Modification

of these surfaces through silanization and chemisorption would appear to be a means for improving the stability of these oxide surfaces, enhancing their compatibility with nonpolar solvents and condensed phase materials, and optimizing rates of interfacial electron transfer.

1.1.2 Factors that Control the Surface Composition of the TCO Electrode

The structure shown in Fig. 1, representing an ideal metal oxide surface, provides a useful platform for understanding metal oxide surfaces. A further, and more realistic, modification to the model would account for the presence of surface hydrolysis products as shown in Fig. 3. Surface hydrolysis critically affects the chemical modification of the TCO surface. Moderate hydrolysis may only break bridging oxygen-metal bonds leaving surface hydroxyl groups. More extensive hydrolysis can lead to fully hydroxylated metal species that may remain physisorbed. The presence of dopants and/or oxygen vacancies, as shown in Fig. 4, can also affect the metal oxide surface by creating sites that can react with adventitious impurities present during, or after, deposition.

Varying degrees of hydroxylation and defect density, as well as the preferential migration of dopants to the near surface region, contribute to the high degree of heterogeneity in electron transfer rates and chemical compatibility commonly observed with oxide electrodes. Hydrolysis products on ITO remain strongly physisorbed (precipitated) to the electrode surface at greater than monolayer coverage, constituting a primary factor for the appearance of electrical ''dead spots'' on the oxide surface [24, 36, 37]. The so-called ''dead spots'' are regions exhibiting poor electroactivity or no electroactivity.

Surface hydrolysis of metal oxide surfaces can be examined by comparison to solution equilibrium constants for hydrolysis and solubility. Indium oxide has a favorable equilibrium constant for hydrolysis [38–40]:

$$In_2O_3 + 3H_2O \longleftrightarrow 2In(OH)_3 \qquad K = 4.3 \times 10^1 \quad (1)$$

Whereas, the fully hydrolyzed In moiety, $In(OH)_3$, has a very low solubility product.

$$In(OH)_3 \longleftrightarrow In^{3+} + 3OH^- \qquad K_{sp} = 1.3 \times 10^{-37} \quad (2)$$

There is also the possibility for incomplete hydrolysis of an indium surface oxide creating the intermediate hydroxylated species, InOOH:

$$In_2O_3 + H_2O \longleftrightarrow 2InOOH \quad (3)$$

This type of surface site may also arise by the nucleophilic attack of water on exposed oxide defects, which serve as sites for dissociative adsorption. In contrast, hydrolysis of tin oxide is significantly less

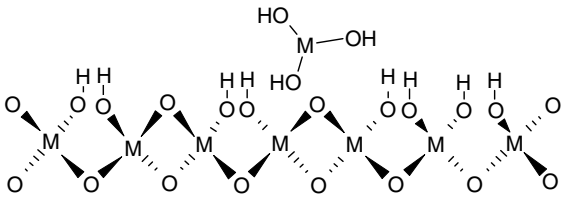

Fig. 3 Schematic view of an oxide surface that has undergone hydrolysis, producing hydroxylated sites, and even physisorbed metal hydroxide, monomers or polymers.

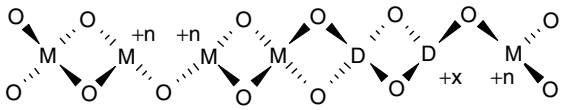

Fig. 4 Schematic view of the near surface region of the oxide thin film with oxygen vacancies, producing electron-rich metal sites and dopant sites of lower stoichiometry, and also creating electron-rich sites.

favored than for indium oxide, at any pH [38, 39]:

$$SnO_2 + 2H_2O \longleftrightarrow Sn(OH)_4 \qquad K = 5.6 \times 10^{-10} \quad (4)$$

While the solubility of tin hydroxide is higher than for indium hydroxide:

$$Sn(OH)_2 \longleftrightarrow Sn^{2+} + 2(OH^-) \qquad K = 1.4 \times 10^{-28} \quad (5)$$

$$Sn(OH)_4 \longleftrightarrow Sn^{4+} + 4(OH^-) \qquad K = 7.2 \times 10^{-14} \quad (6)$$

The typical doped SnO_2 thin film can therefore be expected to show monolayer (but not significantly higher) coverages of hydroxide species. Hydroxide species in excess of monolayer coverage would be expected to be more easily removed from the oxide surface through pretreatment steps.

For titanium oxides and zinc oxides, similar hydrolysis and dissolution processes must be considered [39, 41]:

$$Zn(OH)_2 \longleftrightarrow Zn^{2+} + 2OH^- \qquad K_{sp} = 3 \times 10^{-16} \quad (7)$$

$$Ti(OH)_4 \longleftrightarrow Ti^{4+} + 4OH^- \qquad K_{sp} = 7.94 \times 10^{-54} \quad (8)$$

Chemical modification of these oxides, therefore, needs to take into account the routes to formation and loss of surface hydroxide species playing a key role in determining the surface coverage of the modifier. Rates of electron transfer/charge injection at the modified oxide surface are subsequently affected. Despite the uncertainties in oxide surface composition, several modification protocols have been developed over the last thirty years, which yield improved electrochemical performance of the TCO thin film. Two strategies have continued to be successful at modifying metal oxide electrodes; silanization, covalent bond formation to metal hydroxides, and chemisorption, using functional groups known to either hydrogen bond to M–OH sites and/or to coordinate to metal cation sites.

1.1.3 Chemical Modification of TCO Surfaces Using Silane Chemistries

1.1.3.1 Introduction to Silane Modification

Surface modification of TCO thin films with monofunctional, difunctional, and trifunctional organosilanes arose initially from protocols developed in modifying silica surfaces [42]. The covalent attachment of functional groups to the oxide surface through silanization involves the coupling of the functionalized silane to the metal oxide at hydroxylated sites, through a metal–oxygen–silicon bonded network with the release of one or more ''leaving groups'' as shown in Fig. 5. ''Leaving groups'' are generally chlorides or alkoxides (methoxide or ethoxide) yielding HCl or the corresponding alcohol as by-products.

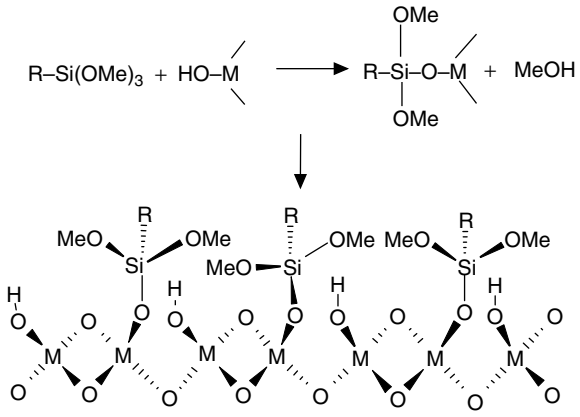

Fig. 5 Schematic view of silane modification of an oxide surface, using (as an example) a tri-methoxy silane. Reaction with only one surface hydroxide site is shown, releasing methanol as the product. Unreacted hydroxide sites remain, as do unreacted alkoxy groups on the silane, which can further cross-link under appropriate conditions.

In the absence of water, silane modifiers can form multiple bonds to the surface creating a clawlike multidentate attachment, Fig. 6(a) [43]. Silanes with multiple leaving groups, however, will generally cross-link during the surface attachment process, or afterward during storage in high humid environments, to form a polymeric, hydrolytically stable layer, as shown in Fig. 6(b). The functional group (R) can be an alkyl or aromatic group terminating with a redox active molecule (ferrocene, viologen, porphyrin, phthalocyanine, etc.) or can simply be tailored to control the wettability of the TCO surface.

It is desirable to start with a surface that has been mildly hydroxylated for surface modification, as opposed to the stoichiometric surface shown in Fig. 1, so that there are sufficient reactive sites for silanization. If the redox chemistry of an attached molecule is to be optimized, it is also desirable to work with monofunctional silanes. In this case, only one

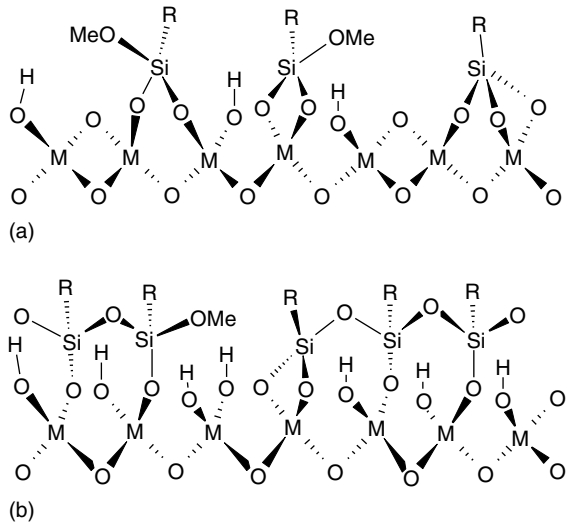

Fig. 6 Schematic view of cross-linking a silane surface modifier as it passes through the (a) multidentate/brush phase to the (b) fully cross-linked phase, with relatively few unreacted M−OH groups left on the oxide surface.

attachment site is created, thereby leaving the tethered redox group in close proximity to the electrode surface and promoting reasonable rates of electron transfer [1]. Control of surface hydroxylation, however, given the tendency of oxides to extensively hydrolyze, is problematic and affects the coverage of redox active groups that can be achieved through silanization reactions. Silane formation on SnO_2 surfaces, where hydrolysis can be more easily controlled appears to be a more advantageous strategy.

Silanization is generally performed in refluxing toluene or benzene with low concentrations of the desired silane. Silanes of the form $X(R2)_2SiR1$ have only one reactive bond and can therefore make only one bond with the metal oxide surface (see Fig. 5). X represents a chloride, methoxy, ethoxy, or other ''leaving group.'' R2 groups are typically small substitutents such as methyl groups, but can be changed to something larger such as phenyl groups to provide steric hindrance and blocking unsilanized surface sites. Large side chains would, however, also sterically reduce the number of silane molecules bound to the oxide. The energy barrier for the surface bonded silane to rehydroxylate, and the metal oxide to ''heal,'' with a bridging oxygen, is extremely low. Therefore, these brushlike phases are generally unstable and nearly all of the brushlike phases reported in the literature are produced with triply reactive silanes reacted under highly controlled dry conditions such that multiple bonds can be made with the surface, as shown in Fig. 6(a). According to Kirkov, there are 2.23×10^{15} Sn−O sites cm^2 on SnO_2 [44, 45], and similar site densities can be expected for ITO and TiO_2. Since not all sites will be uniformly reactive, a maximum surface coverage is approximately 10^{-10} moles cm^{-2} for a brushlike silanized layer with tridentate attachment.

1.1.3.2 Examples of Silane Modification

Trimethoxysilane molecules will covalently attach to ITO following a reflux of the electrode in a 10% (silane:toluene) solution for approximately 30 min [37]. Excess silane can be removed by sonication for 10 min in pure toluene. Water contact angle measurements on such modified surfaces immediately show increased contact angles, consistent with the addition of silane molecules with nonpolar functionality to the surface. On ITO, the contact angle can change from less than 30° before modification, to angles higher than 65° after modification, and even higher if cross-linking of the silane occurs [37, 46]. X-ray photoelectron spectroscopy (XPS) is also used to verify the presence of silicon on the surface. Shepard and Armstrong have measured the electrode interfacial capacitance at tin oxide electrodes modified with a series of silanes [47–50]. The capacitance studies showed the sensitivity of the electrical properties of modified surfaces to variations in reaction conditions during silanization, and to the types of functional groups attached to these surfaces.

Untereker et al. used several methods for creating clawlike brush phase silane layers on SnO_2, TiO_2, and glass [43]. SnO_2 was modified with γ-aminopropyl-triethoxysilane, 3-(2-(aminoethylamino)propyltrimethoxysilane), and β-trichlorosilyl-2-ethylpyridine by exposing the electrodes to 2–10% organosilane solutions in refluxing benzene or xylene under N_2 for up to 12 h. The electrodes were washed with dry benzene. A similar procedure was used for silanizing SnO_2 and TiO_2 at room temperature with lower silane concentrations.

Another brief exposure was performed with 1% organosilane in benzene at 6 °C under argon for 10 s. A more aggressive silanization procedure was used to modify glass with neat organosilane in a sealed tube at 90 °C for 12 h. The authors evaluated their films via XPS to determine thickness and approximate surface coverages.

Finklea and Murray accomplished the silanization of single crystal TiO_2 following a 5 min exposure of the electrodes to 10% silane solutions in either toluene or benzene. Excess silane was removed with fresh solvent, while methanol was found to reduce the silane coverage [51]. The silanes evaluated in these studies were 3-(2-aminoethylamino)-propyltrimethoxysilane, methyltrichlorosilane, and dimethyl-dichlorosilane. XPS surface analysis showed the presence of some cross-linking but could not conclusively characterize the homogeneity of the modified surface. Their photocurrent results indicated that the M−O−Si bond is oxidatively stable to photo-generated holes and, therefore, may provide a useful means of modifying TiO_2 particles for use in dye sensitized solar cells DSSCs. Redox active and photoelectrochemically active metal phthalocyanines were attached to γ-aminopropyltriethoxysilane-modified SnO_2. Tetrasulfonated cobalt and copper phthalocyanines (CoTSPc and CuTSPc) were modified with thionyl chloride, to provide for attachment to the silanized surface via formation of sulfonamide linkages [47, 50].

Phenyl and diphenyl silane-modified ITO surfaces have been used to improve the physical compatibility with Langmuir–Blodgett thin films of phthalocyanine assemblies, where the direct electron transfer of the assembly with the ITO surface was of concern [46].

C_{60} has been tethered to ITO in a self-assembled network by exposing the ITO to basic conditions followed by a reflux in high concentrations of $(MeO)_3Si(CH_2)_3NH_2$ in benzene for half a day [52]. The electrodes were then multiply rinsed before refluxing in a 1-mM solution of C_{60} in benzene for as long as 2 days. This scheme resulted in an ITO-silane-N-C_{60} tethered network and allowed for the formation of an organized C_{60} layer on the ITO surface. Quartz and glass were similarly modified for spectroscopic comparisons. Nearly, all monolayer coverage of C_{60} was determined electrochemically, 1.7×10^{-10} mols cm^{-2}. Reduction of C_{60} in these films is shifted more negatively, indicating a direct interaction between the underlying silyl-amine layer and C_{60}.

1.1.3.3 Silane Modification of Electrodes for Use in Devices

Perfect cross-linking of silane molecules is unlikely in most circumstances due to a mismatch in the lattice spacing between the cross-linked silane layer and the underlying metal oxide substrate. A more accurate picture of a silanized surface would consist of some silane molecules attached via multidentate binding interspersed with cross-linked neighboring silanes as shown in Fig. 6(b). Extensive cross-linking of surface silanes may provide a stable modified surface; however, it also appears to impede electron transfer and, for optimization of solution redox processes, may not be desirable [1, 46].

Marks and coworkers have shown how extensively cross-linked silane monolayers and multilayers can be used to stabilize an electrode and regulate charge injection in a condensed OLED phase [14, 53–55]. Their approach has been to start with silanes functionalized with various redox active

groups and to terminate by functional groups, which can subsequently be converted to new reactive silanes, to produce a layer-by-layer ''self-limiting'' chemistry. Multilayer formation can be well controlled, leading to desired film thicknesses and orientation of the charge transporting core molecules [14]. In general, these modified electrodes show significantly improved performance as anodes in OLEDs, apparently due to the fact that hole injection into the tri-arylamine hole transport layer (which is the core molecule being cross-linked by these silanes), is impeded after modification. This allows for a more balanced injection of both holes and electrons in the device and results in the emissive state forming in the middle of the thin film device [14].

Chlorosilanes are often used to aid in the extensive cross-linking that is desired for the modification of anodes for use in OLED devices. Chlorosilanes liberate HCl as a by-product of silane attachment, which can degrade the TCO surface if low concentrations of base are not added for neutralization. No significant etching of the TCO anode surface has been noted, and surface analysis of the modified electrode generally indicates no entrapped chlorine [14, 51–53].

Silane modification of ITO and SnO_2 electrodes has also been used to create nearly perfect ''blocking'' electrodes, such as thin films where rates of electron transfer are intentionally kept low, so as to provide for measurement in changes in interfacial potential of an additional overlayer, such as a bilayer lipid membrane, during ion transport, pH changes, and so forth. Hillebrandt and Tanaka have evaluated the effects of octyltrimethoxysilane (OTMS), octadecyltrimethoxysilane (ODTMS), and octadecyltrichlorosilane (OTS) on ITO for applications to lipid-membrane-based biological sensors [56–58]. The authors found that the ITO electrodes can be effectively blocked from electron transfer by silanization. Silanization results in more uniform films suitable for the biological sensor platform, with ionic diffusion occurring almost entirely from pinholes in the film. Silanization was accomplished by sonicating ITO substrates in 5 vol% solutions of the silane in dry toluene with 0.5 vol% n-butylamine, followed by 30 min of incubation. Temperatures were held below 293 K for ODTMS and below 280 K for OTMS. Sonication in dry toluene for 2 min removed excess silane. Markovich and Mandler also derivatized ITO with ODTMS but derivatization was performed over a seven-day period [59, 60].

The long alkyl chain length and stability of cross-linked silanized surfaces also allows for their use as masks for patterning and etching TCO substrates. ODTMS has been used as a mask for patterning ITO [61]. Luscombe et al. have used perfluorodecyltrichlorosilane as a mask for etch resists for lithographic processing of ITO surfaces [62].

1.1.4 Modification of TCO Surfaces through Chemisorption of Small Molecules

1.1.4.1 Modification using Small Molecules Containing Carboxylic Acid Functionality

Modification of electrode surfaces through chemisorption has been more in recent reports than silanization, and its discussion here is intended to contrast the strategies used for both types of surface modification. Chemisorption of small molecules to the TCO surface allows for robust modifications occurring over short distances and with relatively strong interactive forces (ΔH = ca. 200 kJ mol^{-1}) through

combinations of electrostatic, H-bonding, and metal ion coordination. Chemisorption processes generally have a high activation barrier for adsorption, may be irreversible, and can "self-limit" at monolayer coverage. Owing to the amphoteric nature of metal oxide surfaces, chemisorption of Lewis acids such as carboxylic acids, aliphatic and aromatic amines, and phosphonic acids are generally successful. Chemisorption typically anchors individual molecules in close proximity to metal cationic sites and may also compete for sites with surface hydrolysis products. Previous work has examined chemisorption to ITO, SnO_2, and TiO_2 surfaces, with most of the studies reporting adsorption of either carboxylic or phosphonic acids or salts.

Carboxylate functionalities have been used repeatedly and successfully as an anchoring group for molecular chemisorption to oxide electrodes proceeding through the formation of an ester linkage to the metal with the loss of water, or through hydrogen-bonding interactions to surface hydroxyl groups. Possible interactions for carboxylic groups are shown in Fig. 7. Binding constants for the carboxylic group for ITO and ATO have been determined to be as high as $8 \times 10^4\ M^{-1}$ [34].

Chemisorption is often as successful as silanization at obtaining monolayer coverages of small molecule modifiers. As an example, Davis and Murray attempted to couple iron porphyrins to amine-terminated silanized SnO_2 surfaces. The authors found that the surface coverage was independent of the apparent extent of surface silanization [63]. Silanized and unsilanized electrodes were soaked in 5 mM porphyrin dissolved in DMF, THF, or pyridine solutions overnight. Porphyrins with pendant carboxylic acid groups produced higher surface coverages (determined by coulometric analysis of the voltammetry of the surface-confined species) on bare, unmodified SnO_2 than seen on SnO_2 electrodes modified with 3-(2-aminoethylamino)propyltrimethoxysilane.

Zotti and coworkers adsorbed several carboxylated ferrocene derivatives on ITO: ferrocene-carboxylic acid (Fc(COOH)), ferrocene-dicarboxylic acid ($Fc(COOH)_2$), and ferrocenylheptanoic acid $Fc(CH_2)_6COOH$ [64]. Fc(COOH) was adsorbed from 1-mM solutions of the molecule in 5/95 ethanol/hexane for as

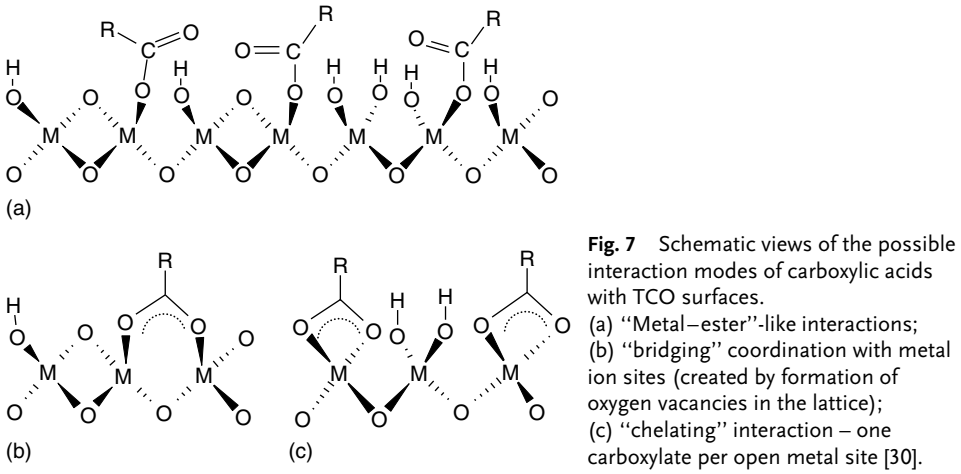

Fig. 7 Schematic views of the possible interaction modes of carboxylic acids with TCO surfaces.
(a) "Metal–ester"-like interactions;
(b) "bridging" coordination with metal ion sites (created by formation of oxygen vacancies in the lattice);
(c) "chelating" interaction – one carboxylate per open metal site [30].

long as 16 h, followed by a rinse with acetonitrile. Higher solution concentrations were found to yield higher surface coverage, following a Langmuir adsorption isotherm, with saturation coverage (ca. 1×10^{-10} mols cm^{-2}) occurring at approximately 10 mM solution concentration. The saturation coverage, however, was 25% of the expected monolayer coverage (4×10^{-10} mols cm^{-2}) based on the geometric area [65]. $Fc(COOH)_2$ was adsorbed from ethanol, while $Fc[(CH_2)_6COOH]$ was adsorbed from hexane. Adsorption of these molecules appears to be kinetically limited. Recent work has shown that time for adsorption is required to remove hydrolysis products (e.g. $In(OH)_3$) or other nonelectroactive species adsorbed to the ITO surface [66].

$Fc(COOH)_2$ has been used successfully to increase electron transfer rates and for enhancing the performance of organic light emitting devices and organic photovoltaics [24, 37]. In addition to modifications of electron transfer rates, carboxylic acid-modified small molecules have been used to introduce dipole fields at the surface of TCO substrates. For example, benzoic acid derivatives have been used to modify the interface dipole at ITO surfaces, attached to the oxide surface via formation of a Langmuir–Blodgett thin film. Changes in work function closely relate to changes in the dipole induced by the derivatized modifiers [67].

Dye molecules possessing carboxylate functionalities have been extensively explored as sensitizers of semiconducting oxide electrodes toward visible light in photoelectrochemical cells [4, 32, 68]. Dye sensitization was first explored as a means of enhancing the photocatalytic properties of TiO_2 [69–72]. Spitler and coworkers investigated dye sensitization of ZnO electrodes using carboxylic acid functionalized dyes [4–6]. The authors found that the photocurrent produced by dye sensitized TiO_2 and ZnO crystals closely resembled the absorption spectrum of the dye, indicating that the dye is in close proximity to the crystal and, upon excitation, injects charge into the semiconductor from energy levels that are relatively unperturbed.

The observation of photocurrent from dye sensitized planar semiconductors led to the evolution of the DSSC, on the basis of extremely high surface area nanoparticulate oxides, usually TiO_2. The most successful dye for sensitization, N3, *cis*-bis(isothiocyanato) bis(2,2′-bipyridyl-4,4′dicarboxylato) ruthenium (II), employs several carboxylic acid groups for adsorption to TiO_2, ZnO, SnO_2, and/or ITO from an ethanol or acetonitrile solution over a several-hour period [32]. Electron injection from the excited state of this dye to the conduction band

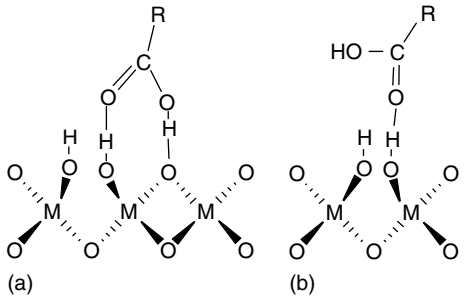

Fig. 8 Schematic views of possible hydrogen-bonding interactions of protonated carboxylic acids to an ideal TCO surface. (a) Interaction mode where the protonated carboxylic acid H-bonds to a bridging oxygen. A hydroxylated metal site also H-bonds to the second carboxylic oxygen. (b) A single hydrogen bond is also plausible.

of the oxide is believed to occur on a femtosecond timescale [73, 74]. Binding constants for the carboxylated dyes assuming an ester linkage are $8 \times 10^4\ M^{-1}$ on SnO_2 from chloroform [73]. A similar carboxylated ruthenium complex has been evaluated on ATO, ITO, TiO_2, and SiO_2 [34]. The authors argue for ester linkages on all substrates except silica. On silica, adsorption occurs through a chelating carboxylato link with a second carboxylate group hydrogen bonding to the surface. Hydrogen-bonding interactions for protonated carboxylic groups to TCO surfaces can also be envisioned as shown in Fig. 8. Notice that physisorption can occur to metal oxide surfaces, which are not hydroxylated, by formation of hydrogen bonds to bridging oxygens.

1.1.4.2 Modification Using Phosphonic Acids and Other Chemisorbing Functionalities

Phosphonic acids are known to chemisorb strongly to oxides such as ITO and have been used to help produce lithographically patterned ITO surfaces [75, 76]. The schematic view of the adsorption of such materials is shown in Fig. 9. Adsorption of hexylferrocene phosphonic acid ($Fc[(CH_2)_6PO(OH)_2]$) has been investigated by Vercelli et al. from ethanol to silanized and unsilanized ITO surfaces [77]. A maximum surface coverage was obtained at 4.2×10^{-10} mols cm^{-2}, approximately four times the surface coverage obtained with the analogous carboxylated ferrocene. Cyclic voltammetry (CV) of the adsorbed ($Fc[(CH_2)_6PO(OH)_2]$) exhibits a symmetric voltammogram about the x-axis (applied potential axis). The high degree of symmetry suggests fast, reversible electron transfer at the interface. Additionally, the modifying molecules were found to be very robust to CV cycling.

An amine derivatized ferrocene molecule, $Fc[CH_2N(CH_3)_2]$, was used to modify ITO, although less successfully than the carboxylic derivatives [64]. Modification with amines tends to create a less robust modification, where the molecules can be easily removed with solvents. CV cycling can also lead to the loss of amine modifiers. This phenomenon is clearly a result of the weaker Lewis base characteristics of the amine for the Lewis acid sites on the metal oxide surface. Han and coworkers, however, were able to design a dense self-assembled monolayer of 1,12-diaminododecane from methanol onto ITO after 60 h of immersion [78]. The terminating amine group allowed for the subsequent addition of a monolayer of phosphomolybdic acid to provide redox active centers. The diaminododecane, at

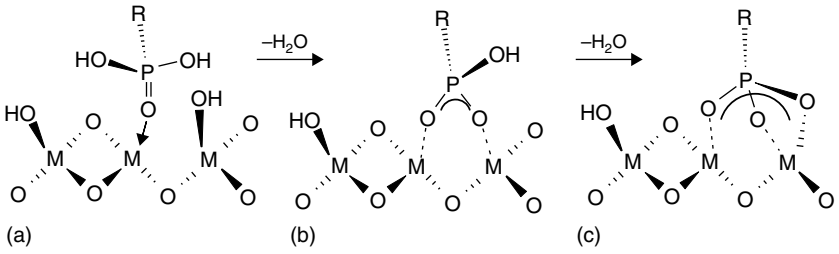

Fig. 9 Schematic views of the possible interaction modes of phosphonic acids with TCO surfaces; (a) monodentate attachment (b) unidentate attachment and (c) multidentate attachment.

6×10^{-10} mols cm^{-2}, provided a platform for one-third as much redox active acid. This protocol may allow for the modification of oxide surfaces through chemisorption to obtain surfaces similar to those obtained through silanization; however, the robustness of this platform was not evaluated.

Cyanuric chloride has been used to modify oxide and graphite electrodes [79]. The linkage, an ether bond through surface hydroxyls, is short and strong, allowing for a robust surface and enhanced electron transfer between the surface and the aromatic terminal group.

Another modification scheme of note is the selective addition of tin-phenoxides on an ITO surface, a process developed by Schwartz and coworkers for the modification of the effective work function of ITO surfaces [13, 80]. Because of the low concentration of tin sites on such surfaces, this modification scheme, which does not modify exposed indium sites, places the functional groups at some distance from each other, a type of modification not afforded by other modification schemes based on covalent bond formation, or chemisorption.

Heme proteins have also been adsorbed to TCO surfaces as ''modifiers'' of their electrochemical properties. These adsorption processes are undoubtedly a combination of electrostatic forces, H-bonding, and metal ion coordination in the TCO surface, and produce reasonably robust and active modifying layers. Cytochrome *C* (cyt *C*) has been the most extensively studied adsorbed heme protein. Hawkridge and coworkers have examined the electrochemical behavior at gold, platinum, and metal oxide electrodes [81]. Electron transfer rates as high as 10^{-2} cm s^{-1} were obtainable at ITO electrodes. Bowden and coworkers have determined that the electron transfer rates are associated with a conformational change of the molecule in the adsorbed state at the electrode surface [82, 83]. Above a certain scan rate, the conformational change can be overcome. More recently, Runge and Saavedra showed that cyt *C* forms a sufficiently stable adsorbed state such that it can be microcontact printed on ITO surfaces, while retaining high electron transfer rates [84].

1.1.5 Conclusions

The modification of TCO surfaces can clearly be used to enhance the electrochemical performance of oxide electrodes. There are, however, issues yet to be resolved regarding the initial surface composition of the oxide, especially for ITO, which prevent realization of the full electrochemical and electronic potential of these electrodes. In some cases, the modification chemistries produce a surface, which is sufficiently robust to be used in various sensor platforms or condensed phase devices. However, it is not yet clear whether long-term stability can be achieved in those cases where the oxide is exposed to solutions that also promote the hydrolysis of the oxide unless an extremely strong covalently bonded network, or chemisorption interaction can be produced. These modification strategies will continue to evolve with the increasing need for viable interfaces between electroactive materials and the metal oxide electrode.

Acknowledgments

Work cited in this review from our laboratories was supported in part by the National Science Foundation (Chemistry); the Office of Naval Research; the

Department of Energy, National Renewable Energy Laboratories Program, Photovoltaics Beyond the Horizon; the Department of Energy, Basic Energy Sciences, and the National Institutes of Health.

References

1. R. W. Murray, Molecular design of electrode surfaces in *Techniques of Chemistry* (Ed.: R. W. Murray), John Wiley & Sons, New York, 1992, pp. 1–48, Vol. 22.
2. F. Decker, J. Melsheimer, H. Gerischer, *Isr. J. Chem.* **1982**, *22*, 195–198.
3. K. Kalyanasundaram, M. Grätzel, *Photosensitization and Photocatalysis Using Inorganic and Organometallic Compounds*, Kluwer Academic Publishers, Boston, 1993.
4. M. A. Ryan, M. T. Spitler, *Langmuir* **1988**, *4*, 861–867.
5. M. T. Spitler, M. Calvin, *J. Chem. Phys.* **1977**, *66*, 4294–4305.
6. M. T. Spitler, M. Calvin, *J. Chem. Phys.* **1977**, *67*, 5193–5200.
7. J. Cui, A. Wang, N. L. Edleman et al., *Adv. Mater.* **2001**, *13*, 1476.
8. J. S. Kim, F. Cacialli, R. Friend, *Thin Solid Films* **2003**, *445*, 358–366.
9. J. S. Kim, R. H. Friend, F. Cacialli, *Synth. Met.* **2000**, *111–112*, 369–372.
10. R. W. Murray, *Acc. Chem. Res.* **1980**, *13*, 135–141.
11. J. J. Pesek, M. T. Matyska, *Interface Sci.* **1997**, *5*, 103–117.
12. K. D. Snell, A. G. Keenan, *Chem. Soc. Rev.* **1979**, *8*, 259–282.
13. A. R. Span, E. L. Bruner, S. L. Bernasek et al., *Langmuir* **2001**, *17*, 948–952.
14. J. E. Malinsky, G. E. Jabbour, S. E. Shaheen et al., *Adv. Mater.* **1999**, *11*, 227–231.
15. R. A. Hatton, S. R. Day, M. A. Chesters et al., *Thin Solid Films* **2001**, *394*, 292–297.
16. C. Ganzorig, K. J. Kwak, K. Yagi et al., *Appl. Phys. Lett.* **2001**, *79*, 272–274.
17. S. Besbes, A. Ltaief, K. Reybier et al., *Synth. Met.* **2003**, *138*, 197–200.
18. P. K. H. Ho, M. Granstrom, R. H. Friend et al., *Adv. Mater.* **1998**, *10*, 769–774.
19. H. L. Hartnagel, A. L. Dawar, A. K. Jain et al., *Semiconducting Transparent Thin Films*, Institute of Physics Publishing, Philadelphia, 1995.
20. R. Hengerer, B. Bolliger, M. Erbudak et al., *Surf. Sci.* **2000**, *460*, 162–169.
21. L.-Q. Wang, D. R. Baer, M. H. Engelhard et al., *Surf. Sci.* **1995**, *344*, 237–250.
22. L.-Q. Wang, K. F. Ferris, A. N. Shultz et al., *Surf. Sci.* **1997**, *380*, 352–364.
23. U. Diebold, *Appl. Phys. A.* **2003**, *76*, 681–687.
24. C. Donley, D. Dunphy, D. Paine et al., *Langmuir* **2002**, *18*, 450–457.
25. J. C. C. Fan, J. B. Goodenough, *J. Appl. Phys.* **1977**, *48*, 3524–3530.
26. N. D. Popovich, S. S. Wong, S. Ufer et al., *J. Electrochem. Soc.* **2003**, *150*, H255–H259.
27. N. D. Popovich, B. K. Yen, S. S. Wong, *Langmuir* **2003**, *19*, 1324–1329.
28. M. Lazzeri, A. Vittadini, A. Selloni, *Phys. Rev. B: Condens. Matter* **2001**, *63*, 155409.
29. M. R. Hoffmann, S. T. Martin, W. Choi et al., *Chem. Rev.* **1995**, *95*, 69–96.
30. K. Kalyanasundaram, M. Gratzel, *Coord. Chem. Rev.* **1998**, *177*, 347–414.
31. M. Fujihira, Y. Satoh, T. Osa, *J. Electroanal. Chem.* **1981**, *126*, 277–281.
32. M. K. Nazeeruddin, R. Humphry-Baker, P. Liska et al., *J. Phys. Chem., B* **2003**, *107*, 8981–8987.
33. M. K. Nazeeruddin, M. Grätzel, *J. Photochem. Photobiol., A* **2001**, *145*, 79–86.
34. T. J. Meyer, G. J. Meyer, B. W. Pfennig et al., *Inorg. Chem.* **1994**, *33*, 3952–3964.
35. J. S. Kim, F. Cacialli, M. Granstrom et al., *Synth. Met.* **1999**, *101*, 111–112.
36. Y. H. Liau, N. F. Scherer, K. Rhodes, *J. Phys. Chem., B.* **2001**, *105*, 3282–3288.
37. C. L. Donley, Interfaces in Organic Electronic Devices: Surface Characterization and Modification and Their Effect on Microstructure in Molecular Assemblies, PhD in Chemistry. 2003, University of Arizona, Tucson.
38. C. F. Baes Jr., R. E. Mesmer, *The Hydrolysis of Cations*, John Wiley & Sons, New York, 1976.
39. D. C. Harris, *Quantitative Chemical Analysis*, W. H. Freeman and Company, New York, 1999.
40. W. F. Linke, *Solubilities: Inorganic and Metal-Organic Compounds*, D. Van Nostrand Co., Inc., New York, 1958.
41. W. F. Linke, *Solubilities: Inorganic and Metal-Organic Compounds*, American Chemical Society, Washington D.C., 1965.

42. J. J. Kirkland, J. J. B. Adams, M. A. van Straten et al., *Anal. Chem.* **1998**, *70*, 4344–4352.
43. D. F. Untereker, J. C. Lennox, L. M. Wier et al., *J. Electroanal. Chem.* **1977**, *81*, 309–318.
44. P. Kirkov, *Electrochim. Acta* **1972**, *17*, 519–532.
45. P. Kirkov, *Electrochim. Acta* **1972**, *17*, 533–547.
46. C. Donley, D. Dunphy, W. J. Doherty et al., *Molecules as Components in Electronic Devices*, American Chemical Society, Washington, 2003.
47. N. R. Armstrong, V. R. Shepard, *J. Electroanal. Chem.* **1980**, *115*, 253–265.
48. N. R. Armstrong, A. W. C. Lin, M. Fujihira et al., *Anal. Chem.* **1976**, *48*, 741–750.
49. N. R. Armstrong, V. R. Shepard, *J. Phys. Chem.* **1981**, *85*, 2965–2970.
50. V. R. Shepard, N. R. Armstrong, *J. Phys. Chem.* **1979**, *83*, 1268–1276.
51. H. O. Finklea, R. W. Murray, *J. Phys. Chem.* **1979**, *83*, 353–358.
52. K. Chen, W. B. Caldwell, C. A. Mirkin, *J. Am. Chem. Soc.* **1993**, *115*, 1193–1194.
53. J. Cui, Q. L. Huang, J. C. G. Veinot et al., *Langmuir* **2002**, *18*, 9958–9970.
54. Q. Huang, G. Evmenenko, P. Dutta et al., *J. Am. Chem. Soc.* **2003**, *125*, 14704–14705.
55. W. Li, Q. Wang, J. Cui et al., *Adv. Mater.* **1999**, *11*, 730–734.
56. H. Hillebrandt, M. Tanaka, *J. Phys. Chem., B* **2001**, *105*, 4270–4276.
57. H. Hillebrandt, M. Tanaka, E. Sackmann, *J. Phys. Chem., B* **2002**, *106*, 477–486.
58. H. Hillebrandt, G. Wiegand, M. Tanaka et al., *Langmuir* **1999**, *15*, 8451–8459.
59. I. Markovich, D. Mandler, *J. Electroanal. Chem.* **2000**, *484*, 194–202.
60. I. Markovich, D. Mandler, *J. Electroanal. Chem.* **2001**, *500*, 453–460.
61. N. L. Jeon, K. Finnie, K. Branshaw et al., *Langmuir* **1997**, *13*, 3382–3391.
62. C. K. Luscombe, H. W. Li, W. T. S. Huck et al., *Langmuir* **2003**, *19*, 5273–5278.
63. D. G. Davis, R. W. Murray, *Anal. Chem.* **1977**, *49*, 194–198.
64. G. Zotti, G. Schiavon, S. Zecchin et al., *Langmuir* **1998**, *14*, 1728–1733.
65. J. Y. Gui, D. A. Stern, F. Lu et al., *J. Electroanal. Chem.* **1991**, *305*, 37–55.
66. C. Carter, M. T. Brumbach, C. Donley et al., manuscript in preparation.
67. M. Carrara, F. Nuesch, L. Zuppiroli, *Synth. Met.* **2001**, *121*, 1633–1634.
68. W.-P. Tai, *Sol. Energy Mater.* **2003**, *76*, 65–73.
69. T. Hoffmann, D. Wrobel, *J. Mol. Struct.* **1998**, *450*, 155–161.
70. P. R. Moses, R. W. Murray, *J. Am. Chem. Soc.* **1976**, *98*, 7435–7436.
71. P. Cuendet, M. Grätzel, M. L. Pelaprat, *J. Electroanal. Chem.* **1984**, *181*, 173–185.
72. P. Cuendet, M. Grätzel, *Bioelectrochem. Bioenerg.* **1986**, *16*, 125–133.
73. A. Hagfeldt, M. Gratzel, *Chem. Rev.* **1995**, *95*, 49–68.
74. A. Hagfeldt, S.-E. Lindquist, M. Gratzel, *Sol. Energy Mater.* **1994**, *32*, 245–257.
75. T. L. Breen, P. M. Fryer, R. W. Nunes et al., *Langmuir* **2002**, *18*, 194–197.
76. T. B. Carmichael, S. J. Vella, A. Afzali, *Langmuir* **2004**, *20*, 5593–5598.
77. B. Vercelli, G. Zotti, G. Schiavon et al., *Langmuir* **2003**, *19*, 9351–9356.
78. S.-Y. Oh, Y.-J. Yun, D.-Y. Kim et al., *Langmuir* **1999**, *15*, 4690–4692.
79. A. M. Yacynych, T. Kuwana, *Anal. Chem.* **1978**, *50*, 640–645.
80. E. L. Bruner, N. Koch, A. R. Span et al., *J. Am. Chem. Soc.* **2002**, *124*, 3192–3193.
81. E. F. Bowden, F. M. Hawkridge, H. N. Blount, *J. Electroanal. Chem.* **1984**, *161*, 355–376.
82. J. L. Willit, E. F. Bowden, *J. Electroanal. Chem.* **1987**, *221*, 265–274.
83. A. El Kasmi, M. C. Leopold, R. Galligan et al., *Electrochem. Commun.* **2002**, *4*, 177–181.
84. A. F. Runge, S. S. Saavedra, *Langmuir* **2003**, *19*, 9418–9424.